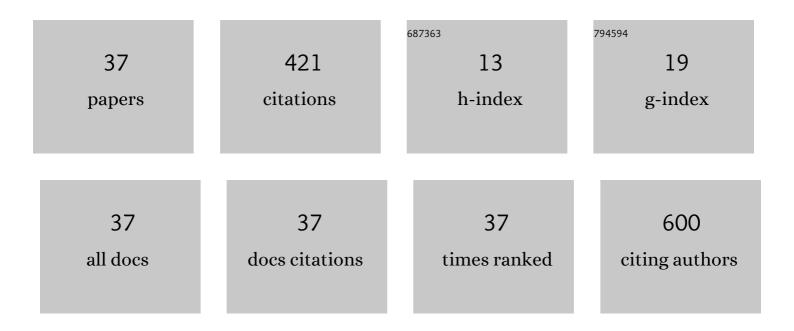
Akira Miyake

List of Publications by Year in descending order

Source: https://exaly.com/author-pdf/5361839/publications.pdf Version: 2024-02-01



AVIDA MIVAVE

#	Article	IF	CITATIONS
1	Eruption style and crystal size distributions: Crystallization of groundmass nanolites in the 2011 Shinmoedake eruption. American Mineralogist, 2017, 102, 2367-2380.	1.9	46
2	Behavior of zircon in the upper-amphibolite to granulite facies schist/migmatite transition, Ryoke metamorphic belt, SW Japan: constraints from the melt inclusions in zircon. Contributions To Mineralogy and Petrology, 2013, 165, 575-591.	3.1	36
3	Discovery of fossil asteroidal ice in primitive meteorite Acfer 094. Science Advances, 2019, 5, eaax5078.	10.3	33
4	Relationship between Raman spectral pattern and crystallographic orientation of a rockâ€forming mineral: a case study of Fo ₈₉ Fa ₁₁ olivine. Journal of Raman Spectroscopy, 2008, 39, 1653-1659.	2.5	29
5	Discovery of moganite in a lunar meteorite as a trace of H ₂ O ice in the Moon's regolith. Science Advances, 2018, 4, eaar4378.	10.3	21
6	An isosymmetric phase transition of orthopyroxene found by high-temperature X-ray diffraction. American Mineralogist, 2008, 93, 1682-1685.	1.9	20
7	Temperature derivatives of elastic wave velocities in plagioclase (An51Â1) above and below the order-disorder transition temperature. American Mineralogist, 2008, 93, 558-564.	1.9	20
8	lsosymmetric structural phase transition of orthoenstatite: Molecular dynamics simulation. American Mineralogist, 2004, 89, 1667-1672.	1.9	19
9	Sillimaniteâ€mullite transformation observed in synchrotron Xâ€ray diffraction experiments. Journal of the American Ceramic Society, 2017, 100, 4928-4937.	3.8	16
10	Composition and <i>I</i> 4/ <i>m</i> P4 ₂ / <i>n</i> phase transition in scapolite solid solutions. American Mineralogist, 2004, 89, 257-265.	1.9	15
11	Effect of the Ionic Size on Thermal Expansion of Low Cordierite by Molecular Dynamics Simulation. Journal of the American Ceramic Society, 2005, 88, 121-126.	3.8	15
12	Stability field of the high-temperature orthorhombic phase in the enstatite-diopside system. American Mineralogist, 2010, 95, 1267-1275.	1.9	15
13	Isochemical breakdown of garnet in orogenic garnet peridotite and its implication to reaction kinetics. Mineralogy and Petrology, 2013, 107, 881-895.	1.1	15
14	Metasomatic PGE mobilization by carbonatitic melt in the mantle: Evidence from sub-μm-scale sulfide–carbonaceous glass inclusion in Tahitian harzburgite xenolith. Chemical Geology, 2017, 475, 87-104.	3.3	14
15	Factors affecting preservation of coesite in ultrahighâ€pressure metamorphic rocks: Insights from <scp>TEM</scp> observations of dislocations within kyanite. Journal of Metamorphic Geology, 2019, 37, 401-414.	3.4	11
16	Effects of Ionic Size in the Tetrahedral and Octahedral Sites on the Thermal Expansion of Low-Temperature Cordierite. Journal of the American Ceramic Society, 2005, 88, 362-366.	3.8	10
17	Sample preparation toward seamless 3D imaging technique from micrometer to nanometer scale. Microscopy (Oxford, England), 2014, 63, i24-i25.	1.5	8
18	Condensation of Glass with Multimetal Nanoparticles: Implications for the Formation Process of GEMS Grains. Astrophysical Journal, 2021, 911, 47.	4.5	7

AKIRA MIYAKE

#	Article	IF	CITATIONS
19	Association of silica phases as geothermobarometer for eucrites: Implication for twoâ€stage thermal metamorphism in the eucritic crust. Meteoritics and Planetary Science, 2021, 56, 1086-1108.	1.6	7
20	Mineralogy of fine-grained matrix, fine-grained rim, chondrule rim, and altered mesostasis of a chondrule in Asuka 12169, one of the least altered CM chondrites. Polar Science, 2021, 29, 100727.	1.2	7
21	Molecular dynamics simulation of high-pressure clinoenstatite Proceedings of the Japan Academy Series B: Physical and Biological Sciences, 1998, 74, 105-109.	3.8	6
22	Clinopyroxene exsolution in wollastonite from Namaqualand granulite, South Africa. American Mineralogist, 2006, 91, 446-450.	1.9	6
23	Molecular dynamics simulations of MgSiO3enstatite and seismic discontinuity in the upper mantle. Geophysical Research Letters, 2005, 32, .	4.0	5
24	Determination of Al/Si order in sillimanite by high angular resolution electron channeling X-ray spectroscopy, and implications for determining peak temperatures of sillimanite. American Mineralogist, 2018, 103, 944-951.	1.9	5
25	Micro-excavation and direct chemical analysis of individual fluid inclusion by cryo-FIB-SEM-EDS: Application to the UHP talc-garnet-chloritoid schist from the Makbal Metamorphic Complex, Kyrgyz Tian-Shan. Geochemical Journal, 2018, 52, 59-67.	1.0	5
26	Howieite in meta-manganese siliceous rocks of Kurosegawa belt, western Kyushu, Japan. Journal of Mineralogical and Petrological Sciences, 2008, 103, 365-370.	0.9	5
27	Three-dimensional observation of GEMS grains: Their high-temperature condensation origin. Geochimica Et Cosmochimica Acta, 2022, 320, 207-222.	3.9	5
28	Experimental synthesis of isochemical kelyphite — a preliminary report. Journal of Mineralogical and Petrological Sciences, 2014, 109, 91-96.	0.9	4
29	Molecular dynamics simulation of Al/Si-ordered plagioclase feldspar. American Mineralogist, 2000, 85, 1159-1163.	1.9	3
30	Significance of an amorphous SiO ₂ phase in a pseudomorph after coesite enclosed in garnet from ultrahighâ€pressure eclogite, Su–Lu Belt, eastern China. Journal of Metamorphic Geology, 2018, 36, 843-854.	3.4	3
31	Formation process of sub-micrometer-sized metasomatic platinum-group element-bearing sulfides in a Tahitian harzburgite xenolith. Canadian Mineralogist, 2020, 58, 99-114.	1.0	3
32	Zoned quartz phenocrysts in supercooled melt inclusions in granulites from continental collision orogens. Island Arc, 2020, 29, e12374.	1.1	2
33	A new occurrence of retrogressed eclogite from the Sanbagawa belt of southwest Japan and its significance. Island Arc, 2019, 28, e12317.	1.1	1
34	Crustal anorthosite formation by deepâ€seated hydrothermal circulation beneath fastâ€spreading axis: Constraints from chronological approach, Sr isotope, and fluid–chromite inclusion investigation. Island Arc, 2021, 30, e12423.	1.1	1
35	Cooling history of a tholeiitic basalt from Funagata Volcano deduced from microstructures of minerals Journal of Mineralogical and Petrological Sciences, 2000, 95, 1-8.	0.9	1
36	Mullite in a buchite from Asama volcano and its sub–micrometric core–rim texture with sillimanite. Journal of Mineralogical and Petrological Sciences, 2018, 113, 198-206.	0.9	1

#	Article	IF	CITATIONS
37	Tracht change of groundmass pyroxene crystals in decompression experiments. Journal of Mineralogical and Petrological Sciences, 2022, 117, n/a.	0.9	1